Electronic Supplementary Material (ESI) for Nanoscale.

Supporting Information

Effect of Thiolate-Ligand Passivation on the Electronic Structure and Optical Absorption Properties of the Ultrathin One and Two-dimensional Gold Nanocrystals

Liang Yang[a], Pu Wang[a]*, Zhenhua Yang[b], Yong Pei[a]*

[a]*Department of Chemistry, Key Laboratory of Environmentally Friendly Chemistry and Applicationics of Ministry of Education, Key Laboratory for Green Organic Synthesis and Application of Hunan Province, Xiangtan University, Hunan Province, Xiangtan 411105, China*

[b]*Key Laboratory of Low Dimensional Materials & Application Technology (Ministryof Education), School of Materials Science and Engineering, Xiangtan University, Xiangtan 411105, Hunan, China*

Email Address: ypei2@xtu.edu.cn

Table S1. The lowest vibrational frequencies of some gold nanoclusters.

Clusters (R = H)	**Frequencies (cm^{-1})**	**Clusters (R = CH_3)**	**Frequencies (cm^{-1})**
$Au_{54}(SH)_{34}$	3.8	$Au_{54}(SCH_3)_{34}$	4.6
$Au_{72}(SH)_{40}$	2.8	$Au_{72}(SCH_3)_{40}$	9.3
$Au_{76}(SH)_{42}$	4.8	$Au_{76}(SCH_3)_{42}$	6.3
$Au_{86}(SH)_{46}$	4.0	$Au_{86}(SCH_3)_{46}$	6.9
$Au_{104}(SH)_{52}$	2.0	$Au_{104}(SCH_3)_{52}$	8.4
$Au_{80}(SH)_{48}$	3.3	$Au_{100}(SH)_{52}$	6.9
$Au_{106}(SH)_{62}$	1.5	$Au_{108}(SH)_{56}$	2.4

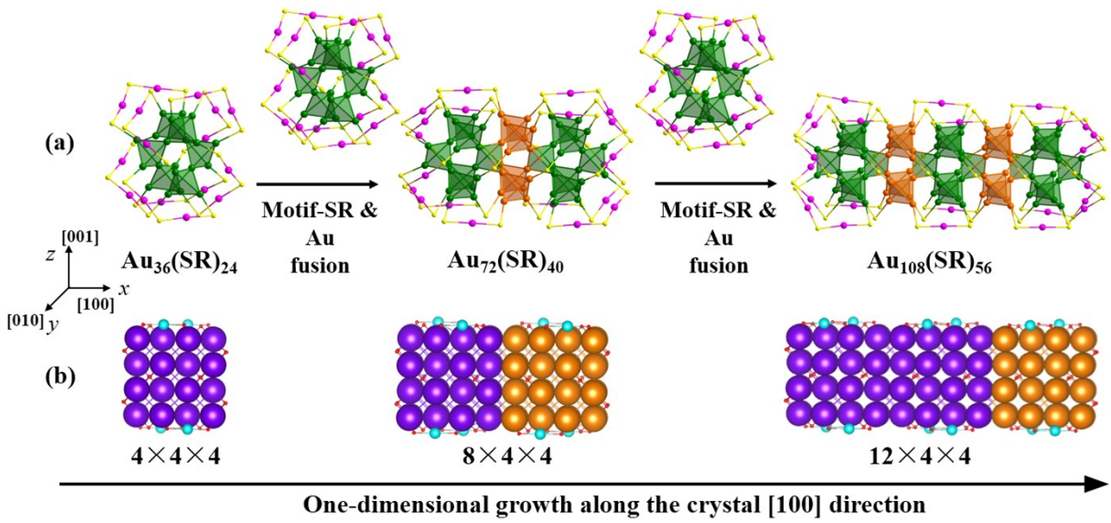

Figure S1 The evolution of geometric structure of the $Au_{36+36n}(SR)_{24+16n}$ cluster along the crystal [100] direction. (a) "COC" structure evolution pattern. (b) Anisotropic layer-by-layer evolution of the fcc gold kernel.

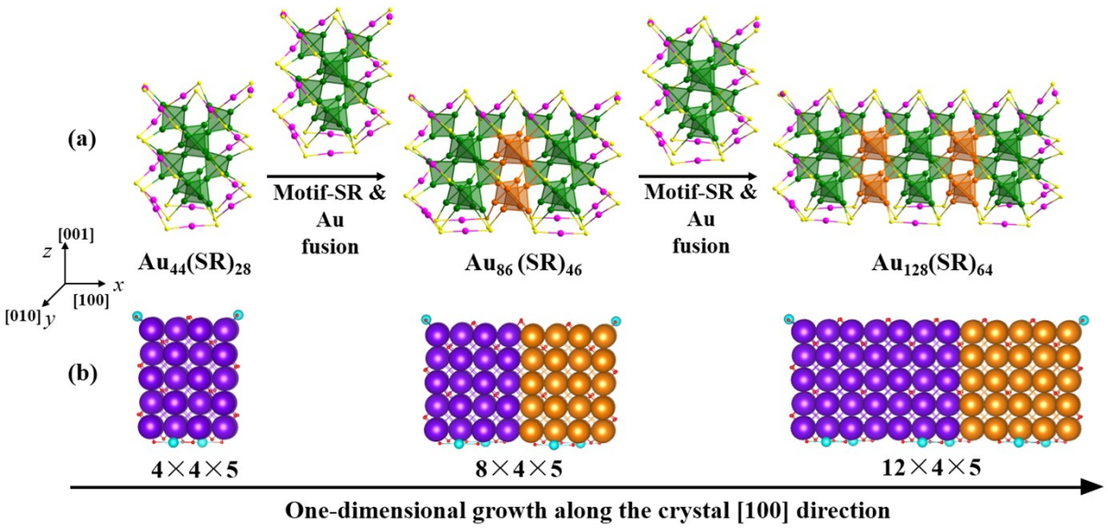

Figure S2 The geometric structure evolution of the $Au_{44+42n}(SR)_{28+18n}$ cluster along the crystal [100] direction. (a) "COC" structure evolution pattern. (b) Anisotropic layer-by-layer evolution of the fcc gold kernel.

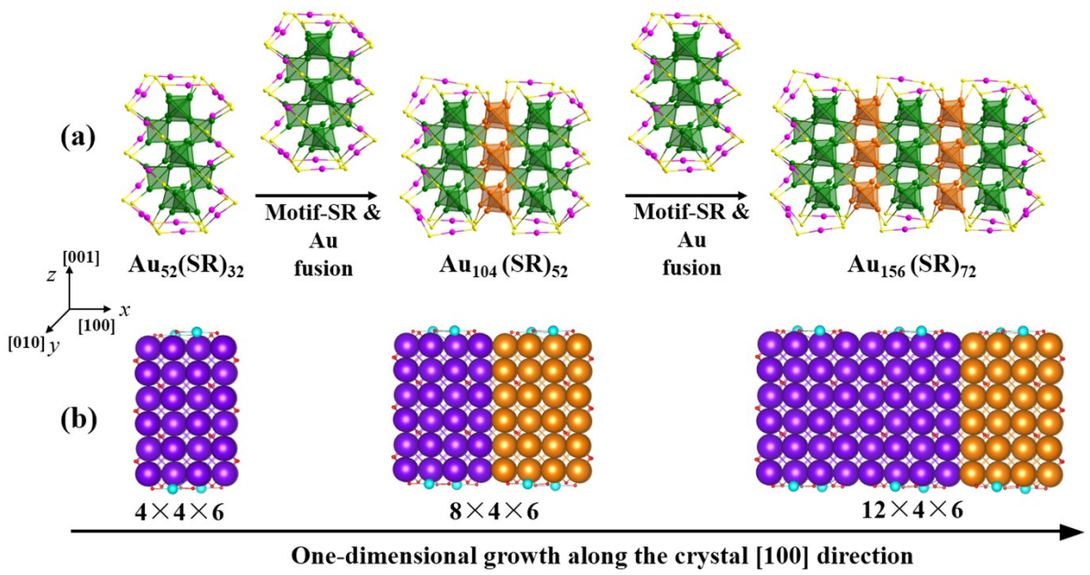

Figure S3 The geometric structure evolution of the $Au_{52+52n}(SR)_{32+20n}$ cluster along the crystal [100] direction. (a) "COC" structure evolution pattern. (b) Anisotropic layer-by-layer evolution of the fcc gold kernel..

Periodic Structures	Front View	Side View
$Au_{28+8n}(SR)_{20+4n}$ ($\infty\times4\times3$)	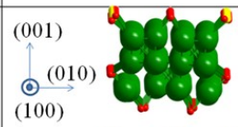	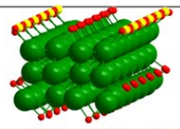 a = 8.727 b = 29.388 c = 28.923
$Au_{36+36n}(SR)_{24+16n}$ ($\infty\times4\times4$)	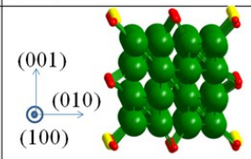	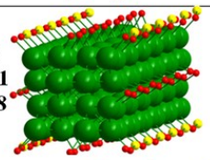 a = 8.584 b = 29.491 c = 29.498
$Au_{44+42n}(SR)_{28+18n}$ ($\infty\times4\times5$)	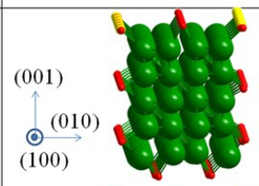	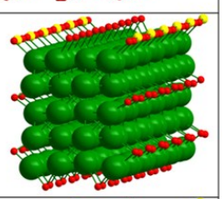 a = 8.575 b = 29.648 c = 29.509
$Au_{52+52n}(SR)_{32+20n}$ ($\infty\times4\times6$)	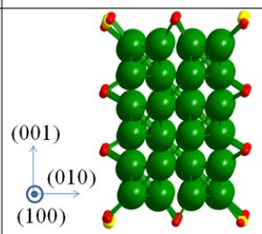	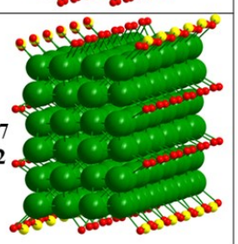 a = 8.536 b = 34.417 c = 29.212
$Au_{52+24n}(SR)_{32+10n}$ ($4\times\infty\times6$)	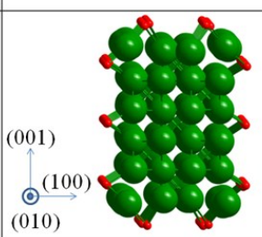	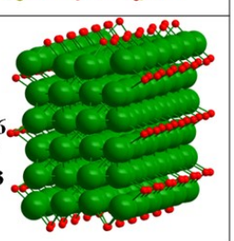 a = 29.526 b = 8.607 c = 31.483

Figure S4. The optimized structure and cell parameters (*a*, *b* and *c*) of the unit cell of the 1D infinite thiolate-passivated gold nanowires. Red ball denotes S atom. The R group is not displayed for clarity.

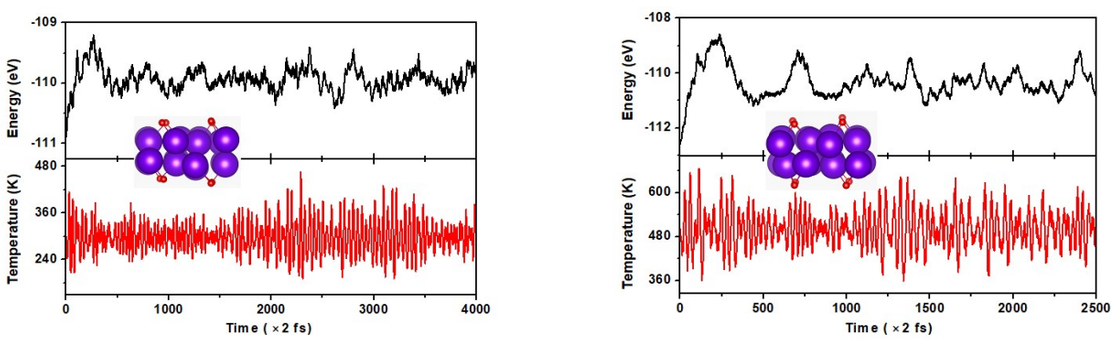

(a) (b)

Figure S5. Evolution of temperature and potential energy against the time in AIMD simulations of ($2\times\infty\times\infty$) periodic system. The simulation is run under 300 K (a) and 500K (b) with a time step of 1 fs, insert is view of the snapshot of gold nanocluster configuration.

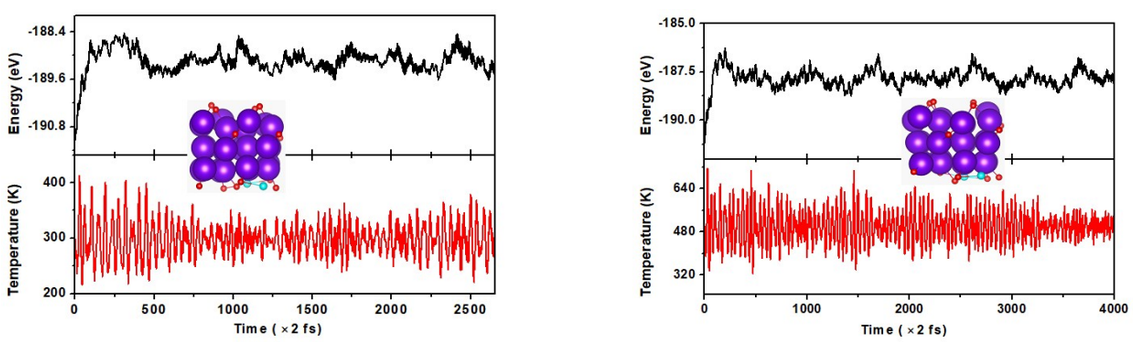

(a) (b)

Figure S6. Evolution of temperature and potential energy against the time in AIMD simulations of ($\infty\times4\times3$) periodic

system. The simulation is run under 300 K (a) and 500K (b) with a time step of 1 fs, insert is view of the snapshot of gold nanocluster configuration. The R groups are not displayed for clarity.

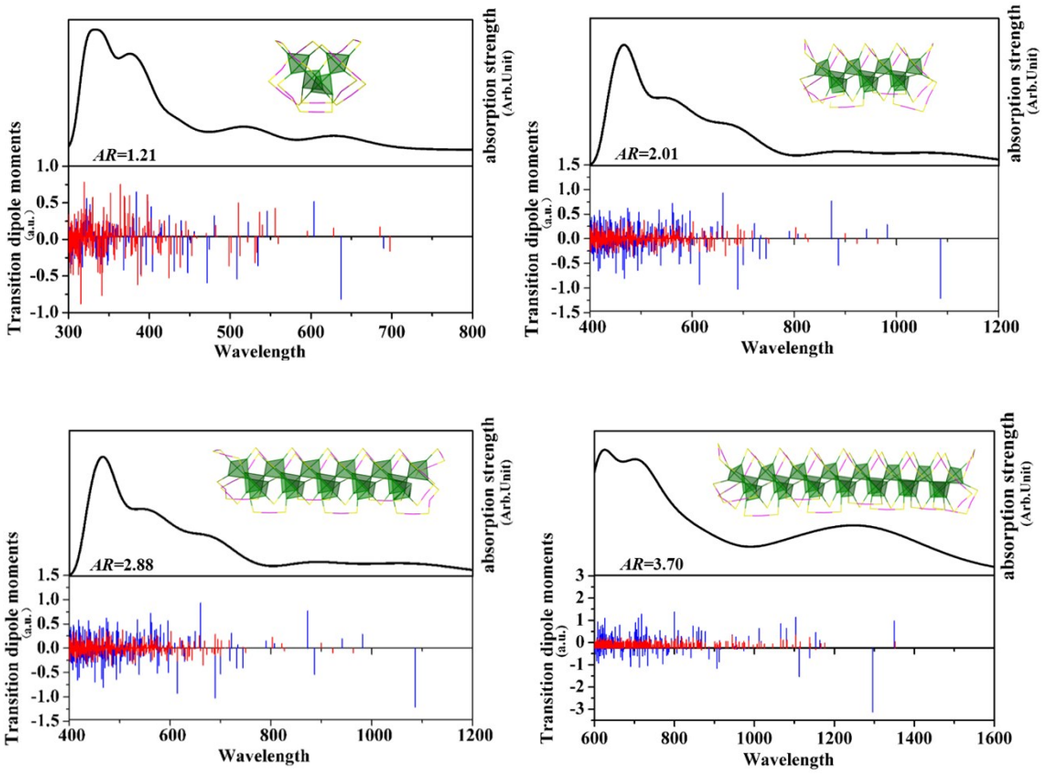

Figure S7 Simulated optical absorption curves and transversal and longitudinal transition dipole moments of $Au_{28}(SR)_{20}$, $Au_{54}(SR)_{34}$, $Au_{80}(SR)_{48}$ and $Au_{106}(SR)_{62}$ clusters with different aspect ratios. Gauss broadening with a width at half-maximum of 0.1 eV is used to fit the optical curve based on the computed excitation energies by TD-DFT method. The blue line represent the transversal transition dipole moment along the crystal [100] direction and the red line represent the longitudinal transition dipole moment along the [001] and [010] directions.

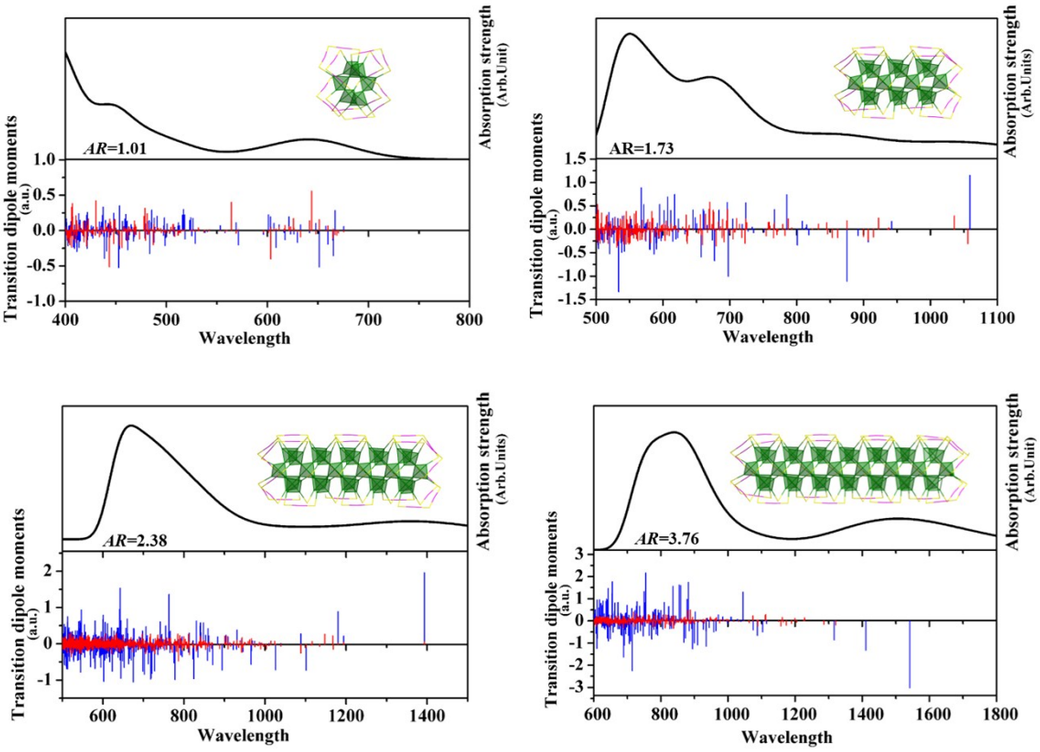

Figure S8 Simulated optical absorption curves and transversal and longitudinal transition dipole moments of $Au_{36}(SR)_{24}$, $Au_{72}(SR)_{40}$, $Au_{108}(SR)_{56}$ and $Au_{144}(SR)_{72}$ clusters with different aspect ratios. The blue line represent the transversal transition dipole moment along the crystal [100] direction and the red line represent the longitudinal transition dipole moment along the crystal [001] and [010] directions.

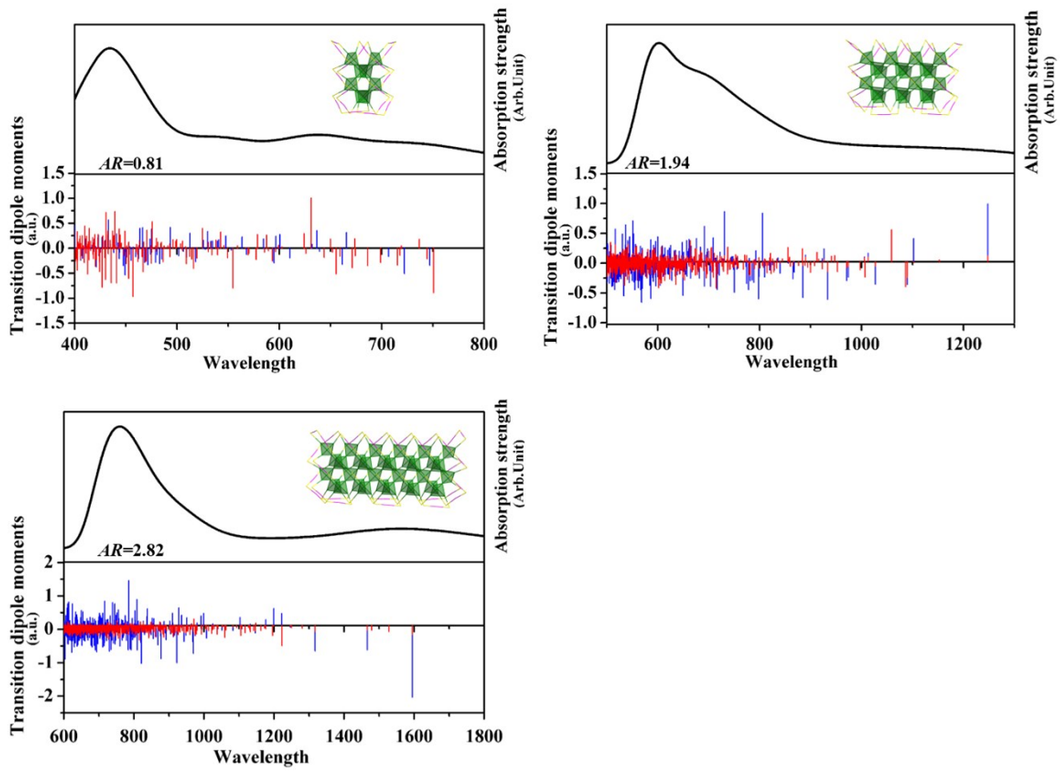

Figure S9 Simulated optical absorption curves and transversal and longitudinal transition dipole moments of $Au_{44}(SR)_{28}$, $Au_{86}(SR)_{46}$, $Au_{128}(SR)_{64}$ clusters with different aspect ratios. The blue line represent the transversal transition dipole moment along the crystal [100] direction and the red line represent the longitudinal transition dipole moment along the crystal [001] and [010] directions.

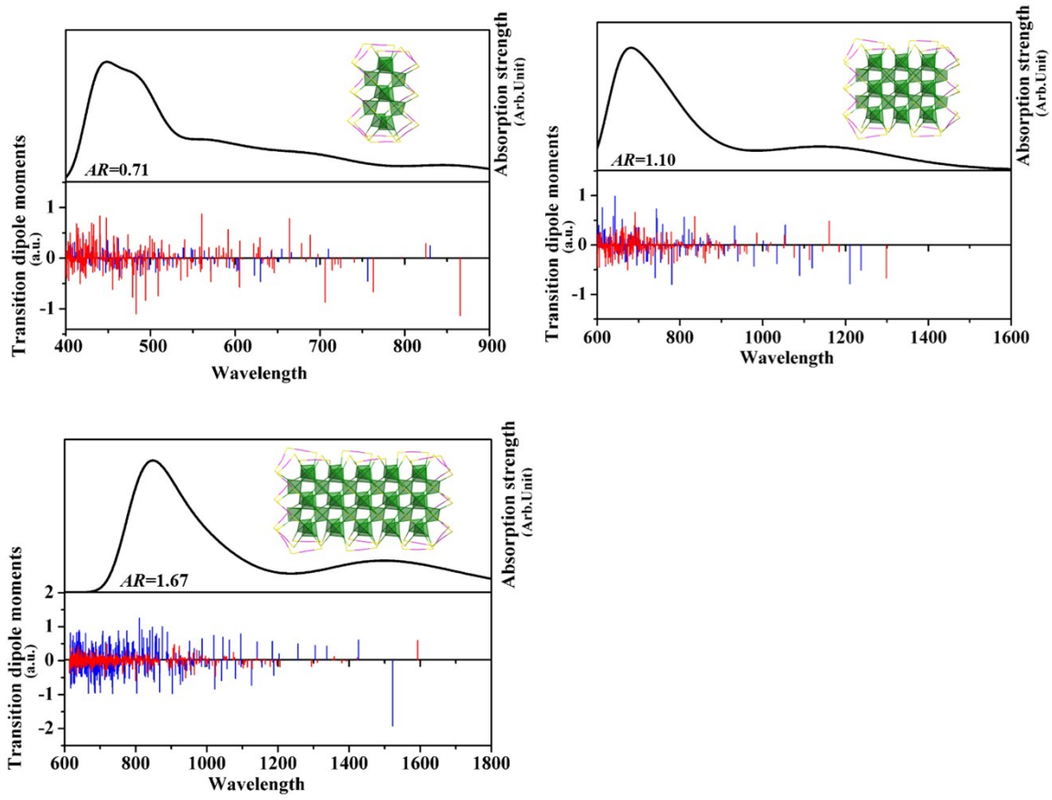

Figure S10 Simulated optical absorption curves and transversal and longitudinal transition dipole moments of $Au_{52}(SR)_{32}$, $Au_{104}(SR)_{52}$, $Au_{156}(SR)_{72}$ clusters with different aspect ratios. The blue line represent the transversal transition dipole moment along the crystal [100] direction and the red line represent the longitudinal transition dipole moment along the crystal [001] and [010] directions.

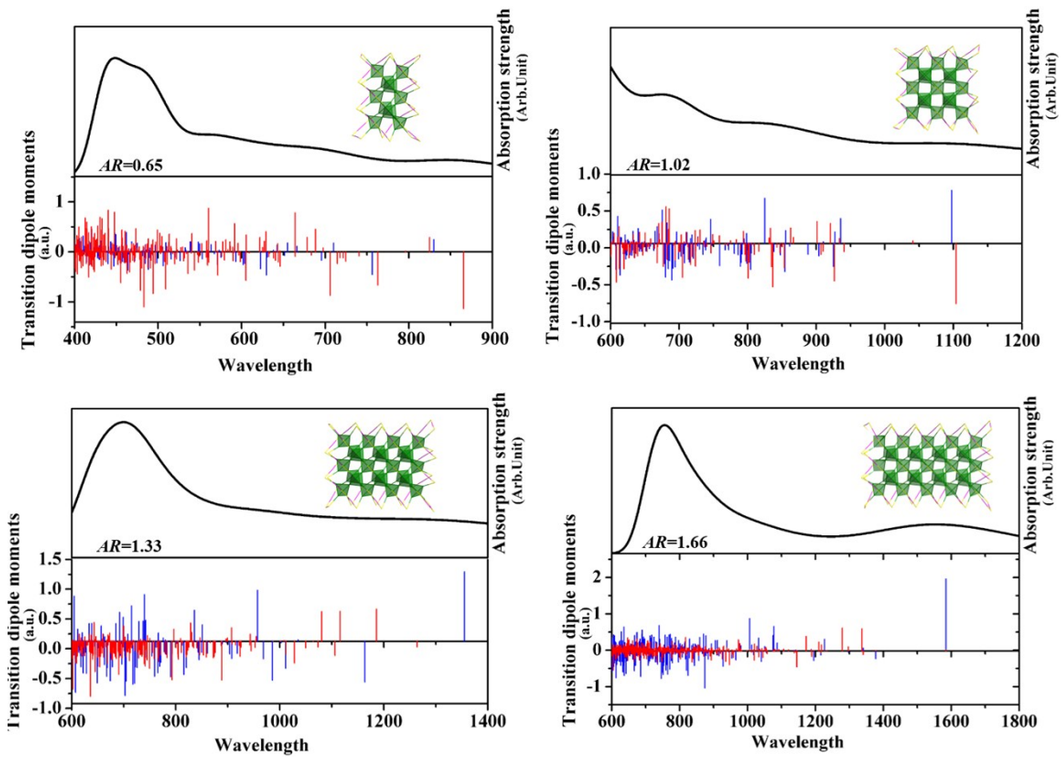

Figure S11 Simulated optical absorption curves and transversal and longitudinal transition dipole moments of $Au_{52}(SR)_{32}$, $Au_{76}(SR)_{42}$, $Au_{100}(SR)_{52}$ and $Au_{124}(SR)_{62}$ clusters with different aspect ratios. The blue line represent the transversal transition dipole moment along the crystal [100] direction and the red line represent the longitudinal transition dipole moment along the crystal [001] and [010] directions.

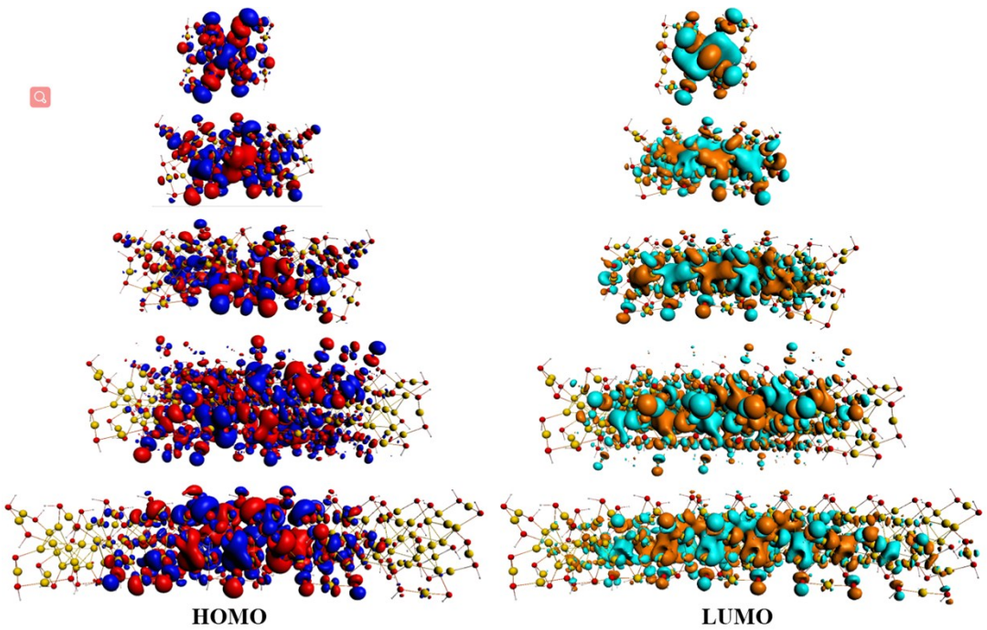

Figure S12 Electronic density diagrams of HOMO and LUMO of $Au_{28}(SR)_{20}$ (AR = 1.21), $Au_{54}(SR)_{34}$ (AR = 2.01), $Au_{80}(SR)_{48}$ (AR = 2.88)， $Au_{106}(SR)_{62}$ (AR = 3.70) and $Au_{132}(SR)_{76}$ (AR = 4.40) clusters. The isovalue used for plotting electronic density is 0.02.

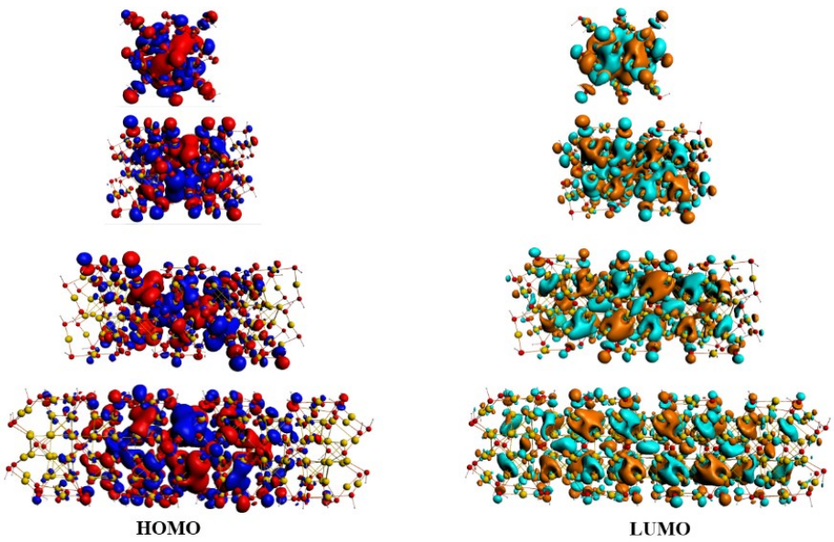

Figure S13 Electronic density diagrams of HOMO and LUMO of $Au_{36}(SR)_{24}$ (AR = 1.01), $Au_{72}(SR)_{40}$ (AR = 1.73), $Au_{108}(SR)_{56}$ (AR = 2.38) and $Au_{144}(SR)_{72}$ (AR = 3.76) clusters.

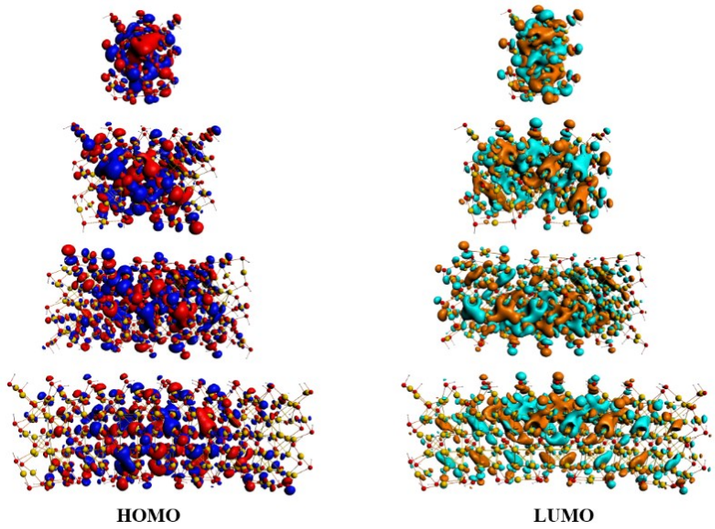

Figure S14 Electronic density diagrams of HOMO and LUMO of $Au_{44}(SR)_{28}$ (AR = 0.81), $Au_{86}(SR)_{46}$ (AR = 1.49), $Au_{128}(SR)_{64}$ (AR = 2.82) and $Au_{170}(SR)_{82}$ (AR = 3.13)clusters.

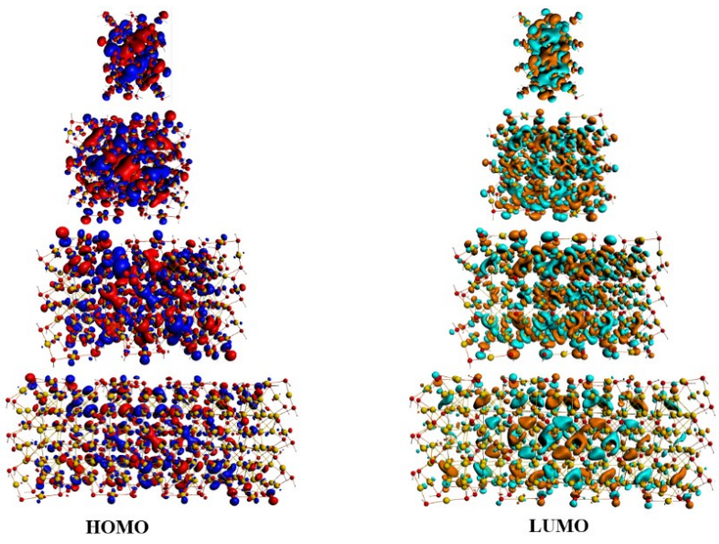

Figure S15 Electronic density diagrams of HOMO and LUMO of $Au_{52}(SR)_{32}$ (AR = 0.71), $Au_{104}(SR)_{52}$ (AR= 1.10), $Au_{156}(SR)_{72}$ (AR = 1.67) and $Au_{208}(SR)_{92}$ (AR = 2.12) clusters.

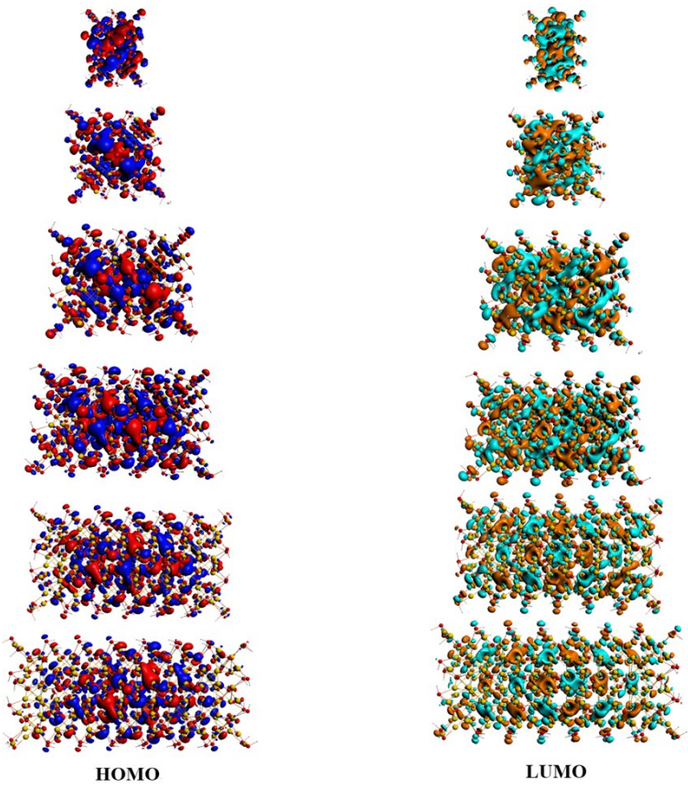

Figure S16 Electronic density diagrams of HOMO and LUMO of $Au_{52}(SR)_{32}$ (AR = 0.65), $Au_{76}(SR)_{42}$ (AR = 1.02), $Au_{100}(SR)_{52}$ (AR = 1.33), $Au_{124}(SR)_{62}$ (AR = 1.66), $Au_{148}(SR)_{72}$ (AR = 2.10) and $Au_{172}(SR)_{82}$ (AR = 2.42) clusters.

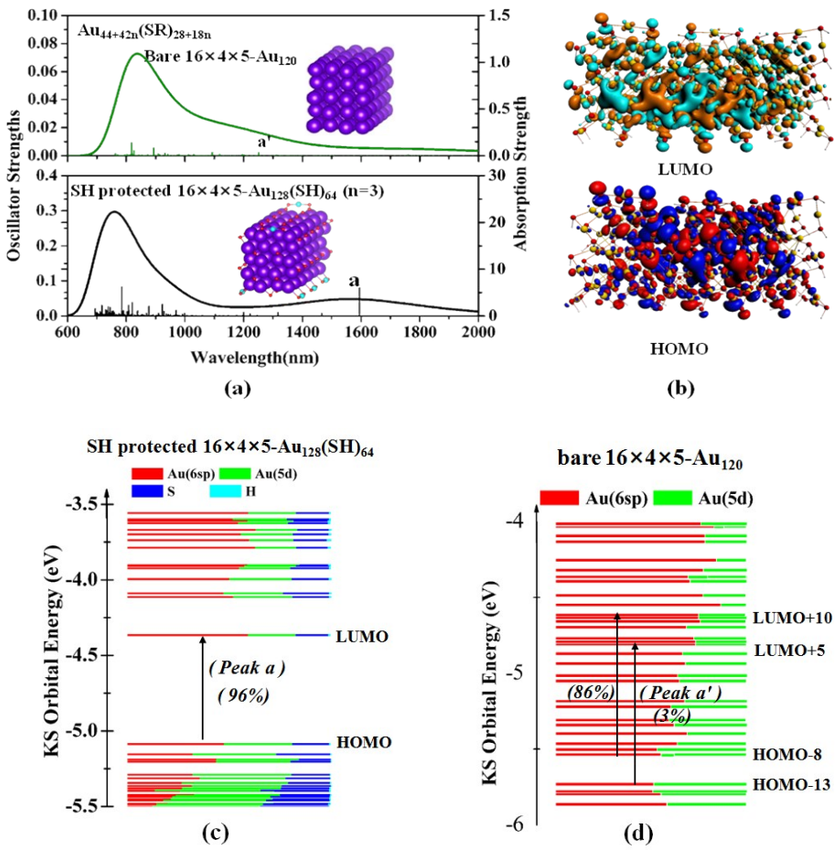

Figure S17 (a) Green line is the simulated UV-via optical absorption curves of Au_{120} cluster (gold kernel in $Au_{128}(SR)_{64}$ cluster) and the black line is the UV-vis curve of $Au_{128}(SR)_{64}$ cluster fitted from the excitation energies computed by TD-DFT. (b) Electronic density of HOMO and LUMO of $Au_{128}(SR)_{64}$ cluster. (c) KS orbital energy levels and atomic orbital component of $Au_{128}(SR)_{64}$ cluster. (d) KS orbital energy levels and atomic orbital component of the Au_{120} cluster.

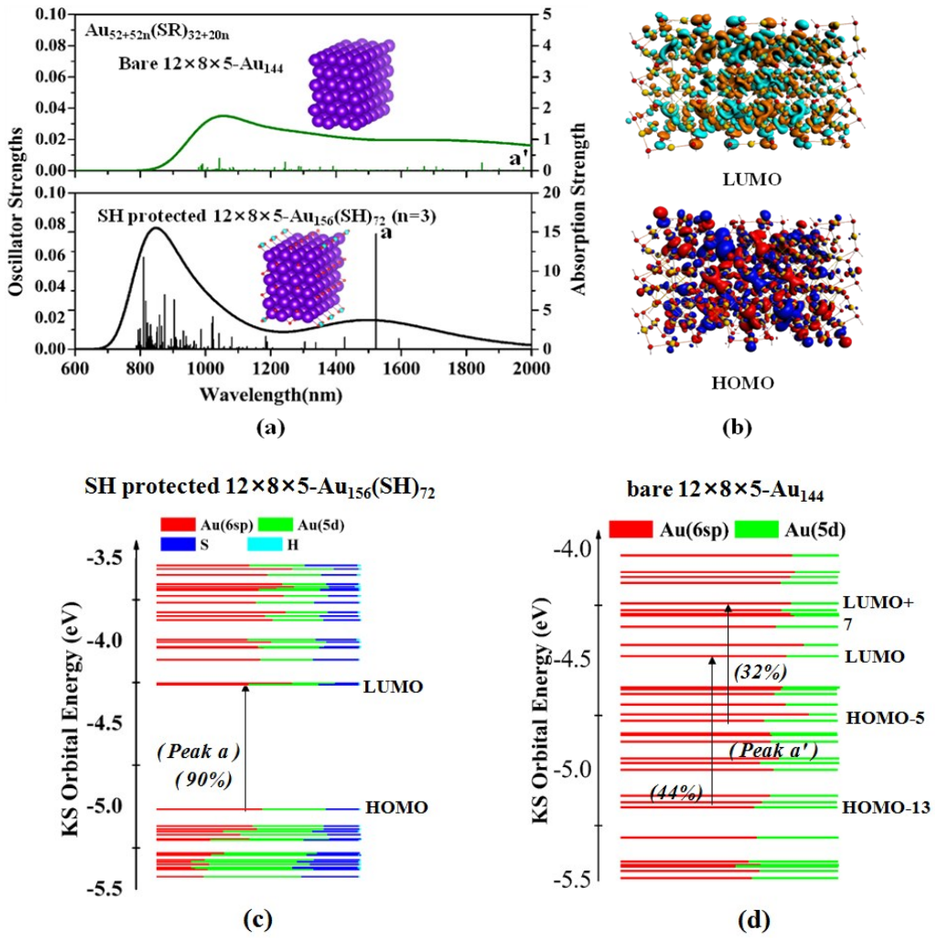

Figure S18 (a) Green line is the simulated UV-via optical absorption curves of Au_{128} cluster cluster (gold kernel in $Au_{156}(SR)_{72}$) and the black line is the UV-vis curve of $Au_{156}(SR)_{72}$ fitted from the excitation energies computed by TD-DFT. (b) Electronic density of HOMO and LUMO of $Au_{156}(SR)_{72}$ cluster. (c) KS orbital energy levels and atomic orbital component of $Au_{156}(SR)_{52}$ cluster. (d) KS orbital energy levels and atomic orbital component of the Au_{144} cluster

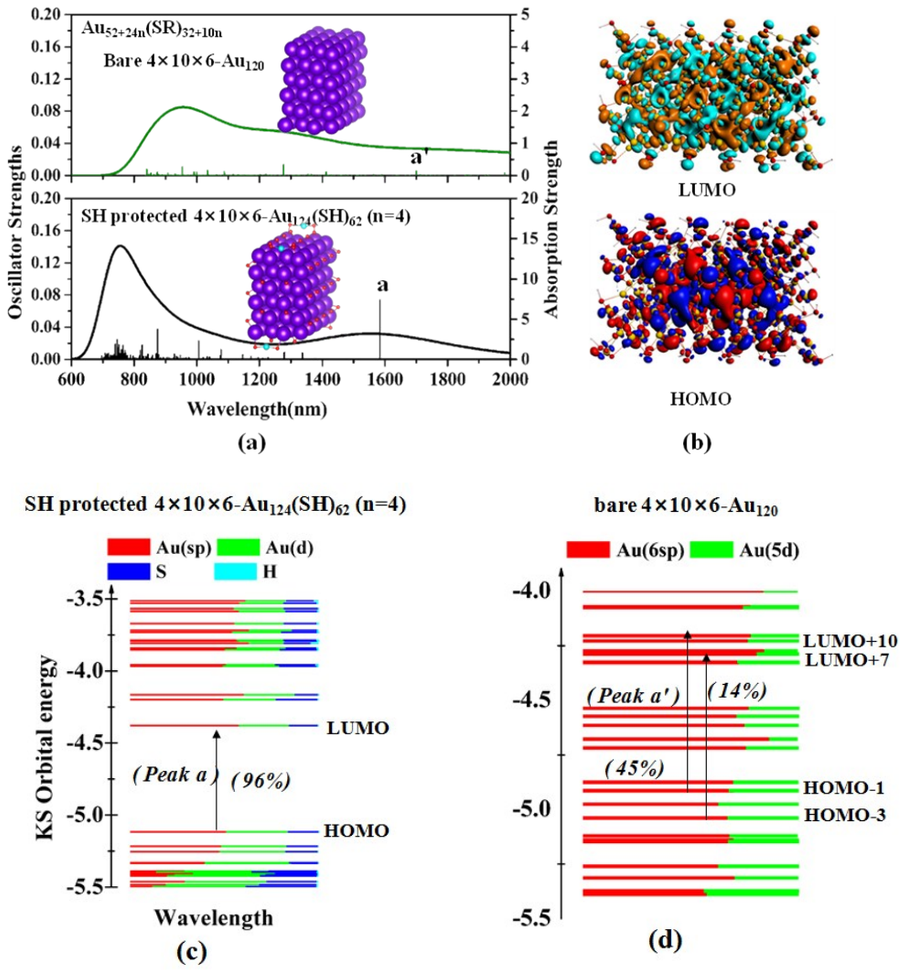

Figure S19 (a) Green line is the simulated UV-via optical absorption curves and of Au_{92} cluster (gold kernel in $Au_{124}(SR)_{62}$ cluster) and the black line is the UV-vis optical absorption curve of $Au_{124}(SR)_{62}$ cluster fitted from the excitation energies computed by TD-DFT. (b) Electronic density of HOMO and LUMO of $Au_{124}(SR)_{62}$ cluster (c) KS orbital energy levels and atomic orbital component of $Au_{124}(SR)_{62}$. (d) KS orbital energy levels and atomic orbital component of the Au_{120} cluster.

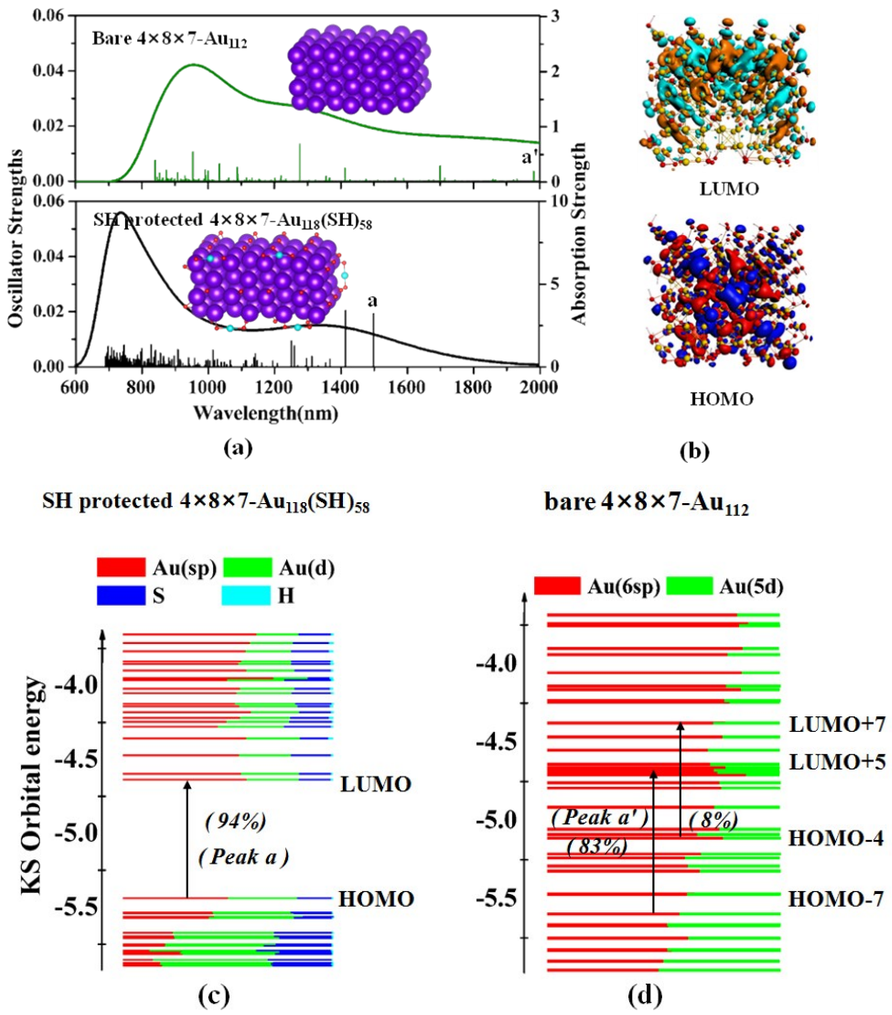

Figure S20 (a) Green line is the simulated UV-via optical absorption curves of Au_{90} cluster (gold kernel in $Au_{118}(SR)_{58}$ cluster) and the black line is the UV-vis optical absorption curve of $Au_{118}(SR)_{58}$ cluster computed by TD-DFT. (b) Electronic density of HOMO and LUMO of $Au_{118}(SR)_{58}$ cluster. (c) KS orbital energy levels and atomic orbital component of $Au_{118}(SR)_{58}$ cluster. (d) KS orbital energy levels and atomic orbital component of the Au_{112} cluster.

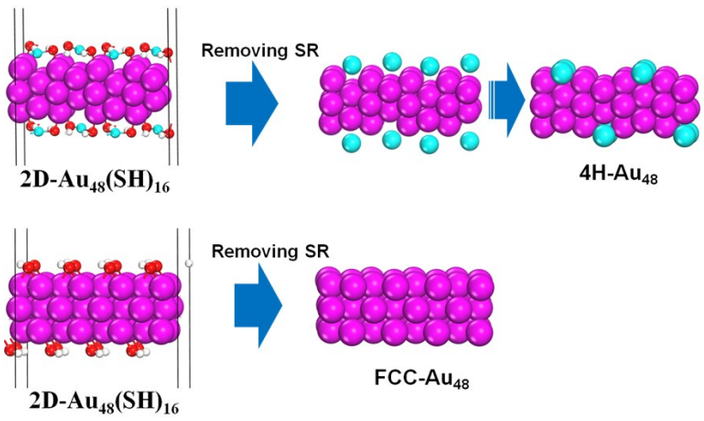

(a)

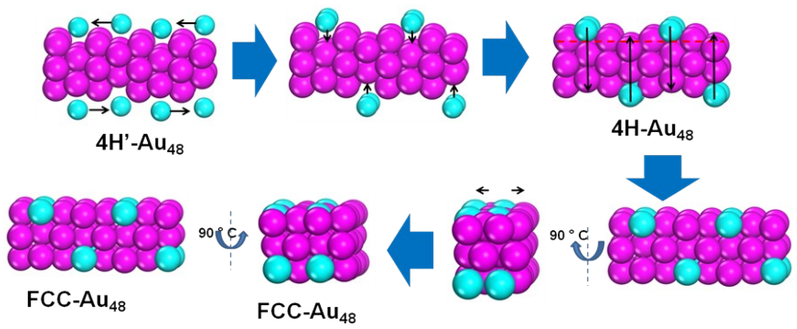

(b)

	4H		FCC	
$Au_{48}(SCH_3)_{16}$	a = 6.00 b = 18.80 c = 36.93	E = 0.00 eV	a = 8.15 b = 16.31 c = 30.00	E = - 2.58 eV
$Au_{64}(SCH_3)_{16}$	a = 6.00 b = 18.80 c = 45.57	E = 0.00 eV	a = 8.15 b = 16.31 c = 30.00	E = - 2.98 eV
$Au_{80}(SCH_3)_{16}$	a = 6.00 b = 18.80 c = 45.57	E = 0.00 eV	a = 8.15 b = 16.31 c = 40.19	E = - 1.37 eV

(c)

Figure S21. (a) Schematic illustration of difference of 4H-type and fcc-type 2D infinite $Au_{48}(SR)_{16}$ gold nanostructures (three-layer gold atoms). (b) The transformation from the 4H phase to FCC phase. (c) A comparison of the optimized geometric structures and relative stabilities of the 2D fcc-structured gold nanosheets and the 4H-type gold nanosheets.

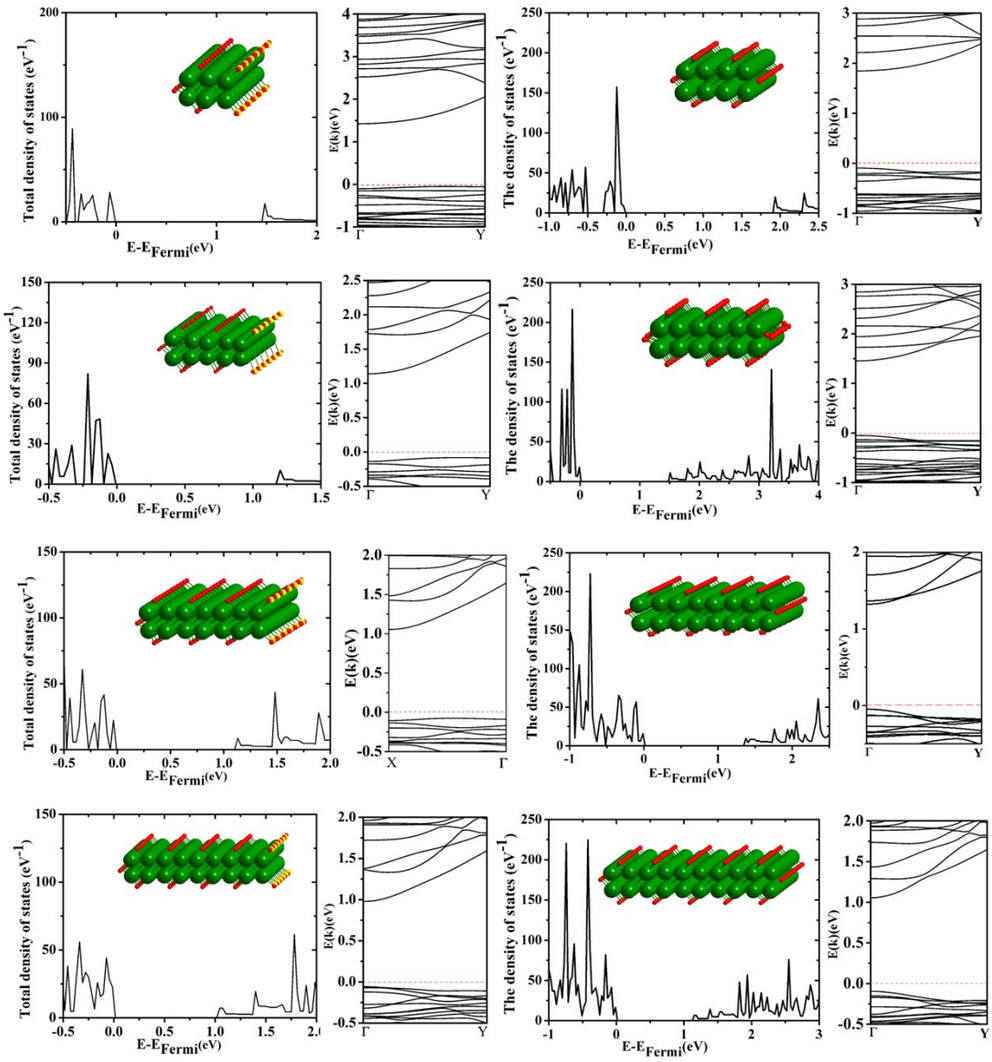

Figure S22 Total electronic density of states (left) and band structure (right) of the thiolate protected 2×3×∞, 2×4×∞, 2×5×∞, 2×6×∞, 2×7×∞, 2×8×∞, 2×9×∞ and 2×10×∞ 1D gold superstructures.

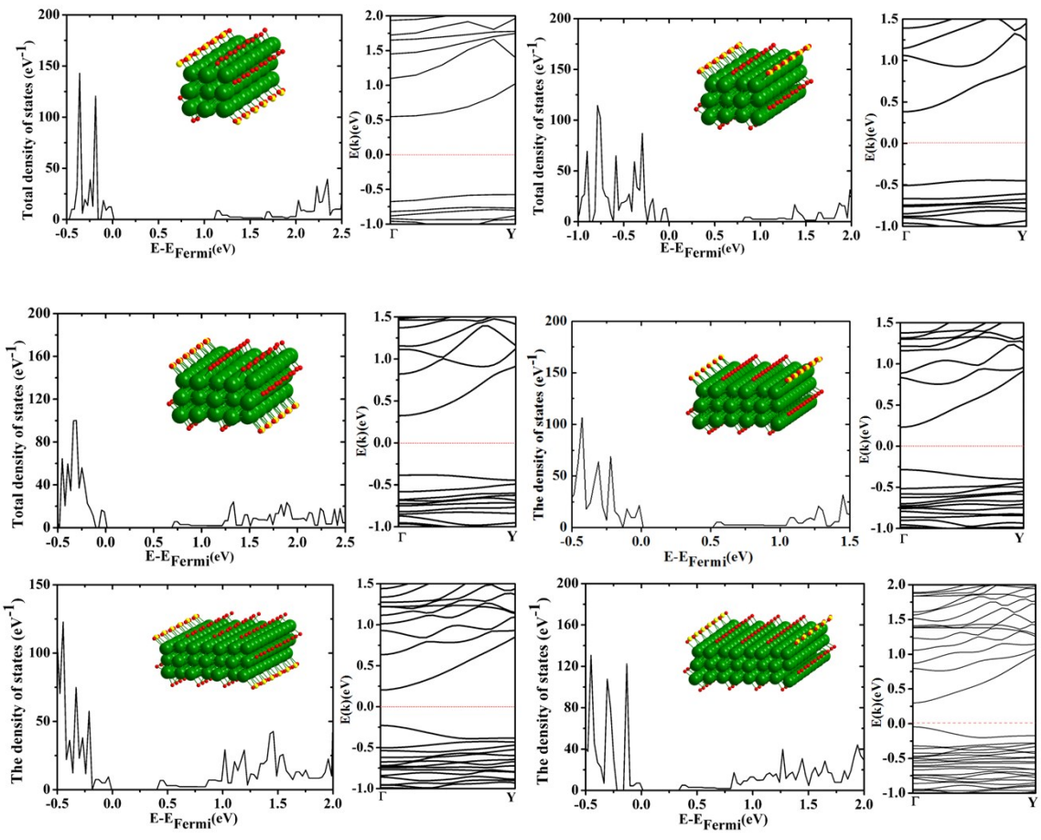

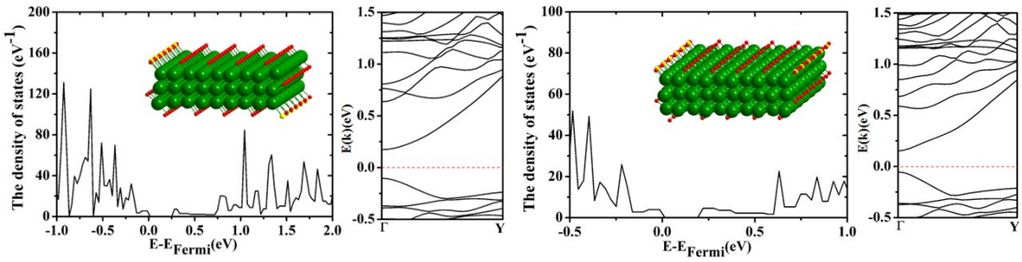

Figure S23 Total electronic density of states (left) and band structure (right) of the thiolate protected 3×3×∞, 3×4×∞, 3×5×∞, 3×6×∞, 3×7×∞, 3×8×∞, 3×9×∞, 3×10×∞ 1D gold superstructures.

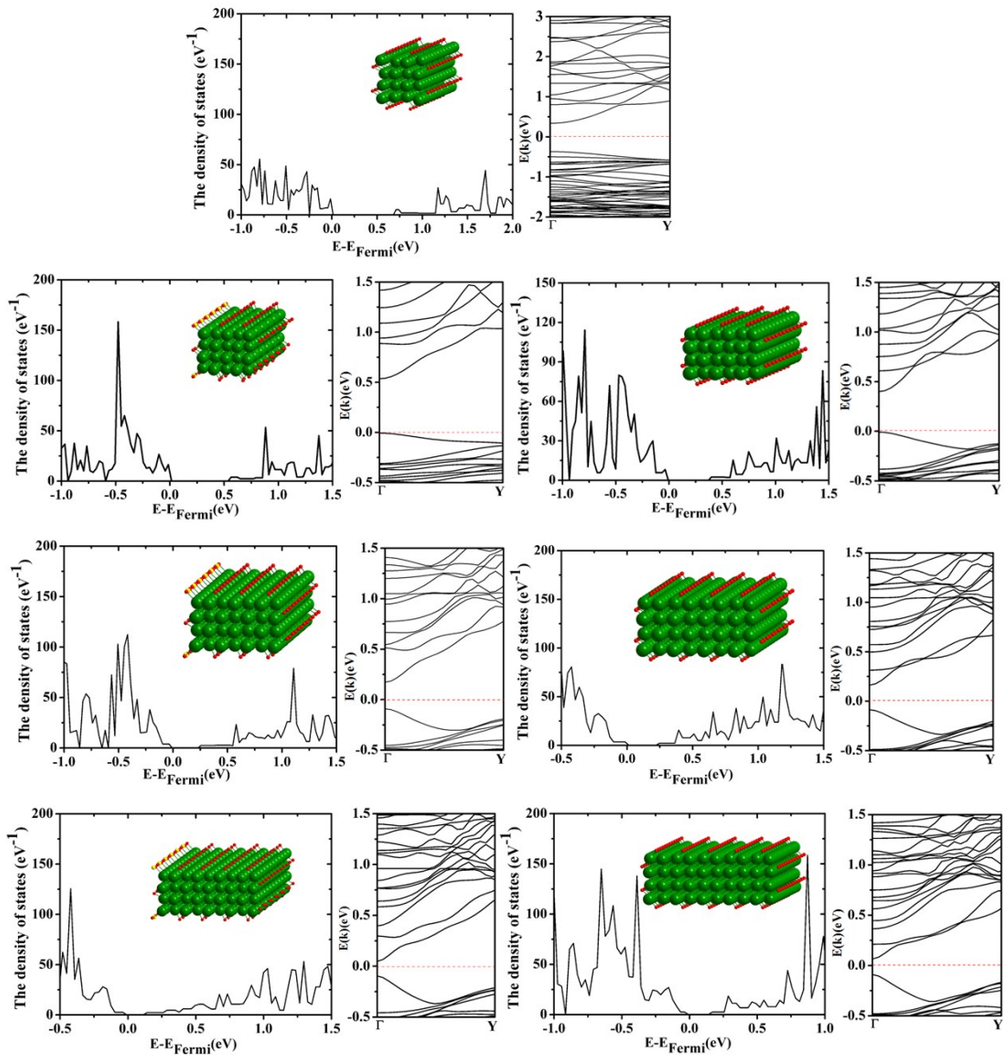

Figure S24 Total electronic density of states (left) and band structure (right) of the thiolate protected 4×4×∞, 4×5×∞, 4×6×∞, 4×7×∞, 4×8×∞, 4×9×∞, 4×10×∞ 1D gold superstructures.

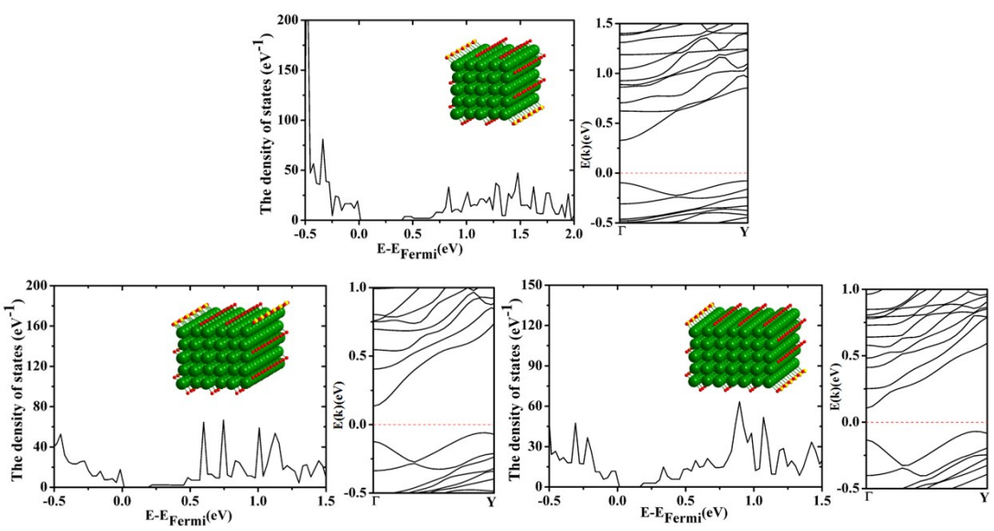

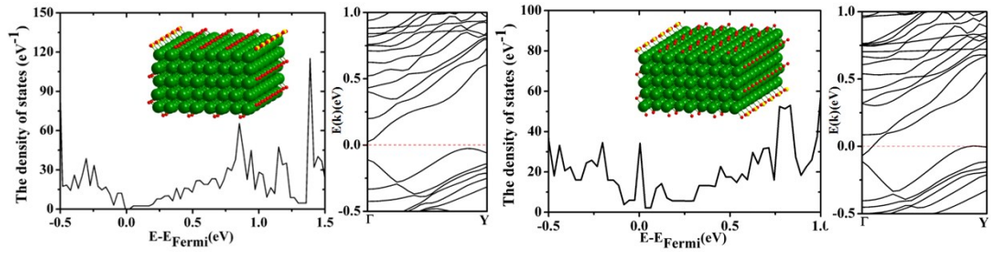

Figure S25 Total electronic density of states (left) and band structure (right) of the thiolate protected 5×5×∞, 5×6×∞, 5×7×∞, 5×8×∞, 5×9×∞ 1D gold superstructures.

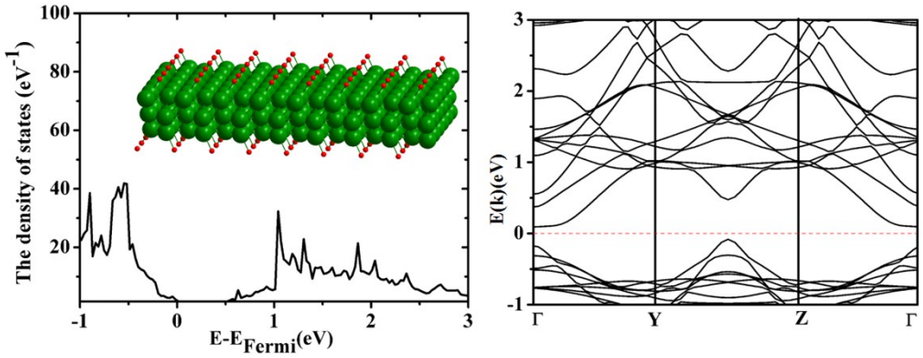

Figure S26 Total electronic density of states (left) and band structure (right) of the 3×∞×∞ 2D infinite gold nanosheet.

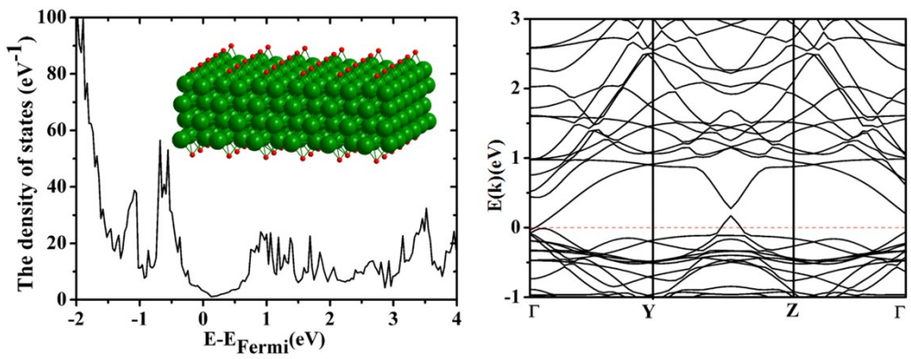

Figure S27 Total electronic density of states (left) and band structure (right) of the 4×∞×∞ 2D infinite gold nanosheet.

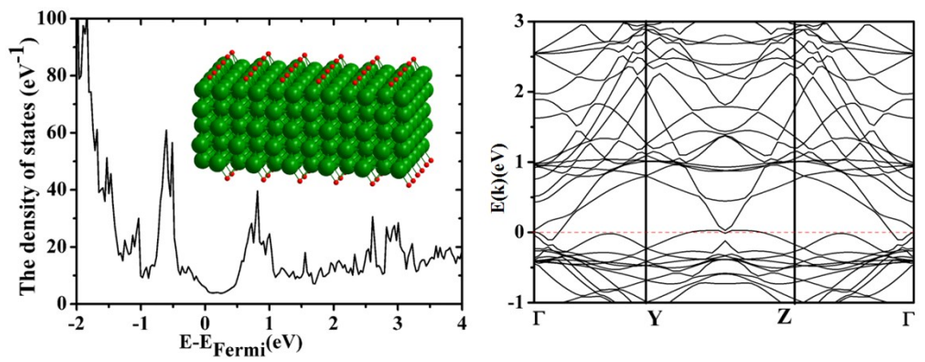

Figure S28 Total electronic density of states (left) and band structure (right) of the 5×∞×∞ 2D infinite gold nanosheet.